The composition of mantle plumes and the deep Earth

Earth and Planetary Science Letters 444 (2016) 13–25

Contents lists available at ScienceDirect

Earth and Planetary Science Letters

www.elsevier.com/locate/epsl

The composition of mantle plumes and the deep Earth

Alan R. Hastie [a,*], J. Godfrey Fitton [b], Andrew C. Kerr [c], Iain McDonald [c], Antje Schwindrofska [d,e], Kaj Hoernle [d,e]

[a] School of Geography, Earth and Environmental Sciences, University of Birmingham, Edgbaston, Birmingham B15 2TT, UK [1]
[b] School of GeoSciences, University of Edinburgh, King's Buildings, Edinburgh, EH9 3JW, UK
[c] School of Earth and Ocean Sciences, Cardiff University, Main Building, Park Place, Cardiff, CF10 3AT, UK
[d] GEOMAR Helmholtz Centre for Ocean Research Kiel, Wischhofstr. 1-3, D-24148 Kiel, Germany
[e] Institute of Geosciences, Christian-Albrechts-University of Kiel, Ludewig-Meyn-Strasse 10, 24118 Kiel, Germany

ARTICLE INFO

Article history:
Received 11 January 2016
Received in revised form 7 March 2016
Accepted 12 March 2016
Available online xxxx
Editor: B. Marty

Keywords:
primary magma
mantle plume
Caribbean oceanic plateau
Ontong Java Plateau
non-chondritic Bulk Silicate Earth (BSE)
normalising factor

ABSTRACT

Determining the composition and geochemical diversity of Earth's deep mantle and subsequent ascending mantle plumes is vital so that we can better understand how the Earth's primitive mantle reservoirs initially formed and how they have evolved over the last 4.6 billion years. Further data on the composition of mantle plumes, which generate voluminous eruptions on the planet's surface, are also essential to fully understand the evolution of the Earth's hydrosphere and atmosphere with links to surface environmental changes that may have led to mass extinction events. Here we present new major and trace element and Sr–Nd–Pb–Hf isotope data on basalts from Curacao, part of the Caribbean large igneous province. From these and literature data, we calculate combined major and trace element compositions for the mantle plumes that generated the Caribbean and Ontong Java large igneous provinces and use mass balance to determine the composition of the Earth's lower mantle. Incompatible element and isotope results indicate that mantle plumes have broadly distinctive depleted and enriched compositions that, in addition to the numerous mantle reservoirs already proposed in the literature, represent large planetary-scale geochemical heterogeneity in the Earth's deep mantle that are similar to non-chondritic Bulk Silicate Earth compositions.

1. Introduction

The composition and geochemical diversity of Earth's deep mantle and ascending mantle plumes have been studied for ~60 years and are still intensely debated (e.g., Ringwood, 1962; Schilling, 1973; Hofmann and White, 1982; Sun, 1982; Zindler and Hart, 1986; Hart, 1988; Salters and Zindler, 1995; Phipps Morgan and Morgan, 1999; Salters and Stracke, 2004; Sobolev et al., 2005; Workman and Hart, 2005; Boyet and Carlson, 2006; Caro and Bourdon, 2010; Jackson and Jellinek, 2013; Coogan et al., 2014; Hoernle et al., 2015; Trela et al., 2015). To identify the geochemical makeup of the planet's lower silicate mantle is vital to better understand how Earth's mantle reservoirs and those of extra-terrestrial bodies, initially formed, and evolved, over the last ~4.6 billion years. Equally, determining the composition of mantle plumes, which generate voluminous eruptions on the planet's surface, is essential for Earth scientists to fully understand the evolution of Earth's hydrosphere and atmosphere and possible mechanisms for mass extinction events (e.g., Coffin and Eldholm, 1994; Wignall, 2001; White and Saunders, 2005; Campbell, 2007; Reichow et al., 2009; Kerr, 1998, 2014).

The common practice of normalising mantle-derived basic igneous rocks to chondritic primitive mantle (Bulk Silicate Earth) is useful for highlighting characteristic elemental depletions and enrichments that can not only resolve petrogenetic processes but can also help elucidate the mechanisms responsible for generating geochemically distinct mantle source reservoirs. Nevertheless, the existence of a chondritic primitive mantle reservoir(s) within the modern Earth is controversial with many studies suggesting that it does not, and may never have, existed (e.g., Hofmann and White, 1982; Hart, 1988; Boyet and Carlson, 2006; Caro and Bourdon, 2010; Jackson et al., 2010; Jackson and Jellinek, 2013). Salters and Stracke (2004) and Workman and Hart (2005) provide several compositions for the depleted mid-ocean ridge basalt (MORB) source reservoir in the upper mantle that have been used by others to geochemically model the formation of upper mantle-derived mag-

* Corresponding author.
E-mail addresses: a.r.hastie@bham.ac.uk (A.R. Hastie), godfrey.fitton@ed.ac.uk (J.G. Fitton), KerrA@cardiff.ac.uk (A.C. Kerr), Mcdonaldl1@cardiff.ac.uk (I. McDonald), khoernle@geomar.de (K. Hoernle).
[1] Present address.

http://dx.doi.org/10.1016/j.epsl.2016.03.023

mas. Similarly, determining a more accurate composition of deep mantle plume source regions would make studies into the petrogenesis of mantle plume-derived rocks and intraplate volcanism more robust (e.g., Fitton and Godard, 2004; Hastie and Kerr, 2010; Loewen et al., 2013; Jackson et al., 2015).

This paper presents new major and trace element and Sr–Nd–Hf–Pb radiogenic isotope data for primitive oceanic plateau lavas from the island of Curaçao, Dutch Antilles, southern Caribbean. The new Curaçao data will be compared with the composition of samples from the Ontong Java Plateau (OJP) in the western Pacific (Fitton and Godard, 2004) to determine the composition of Caribbean oceanic plateau (COP) and OJP primary mantle plume magmas. The aim of this study is to use the COP and OJP primary magmas to calculate the composition of the COP and OJP mantle plume source regions. These primary magma and mantle plume reservoir compositions can subsequently be used: (1) to assess the composition of the deep Earth and how the lower mantle may have evolved through geological time, (2) in geochemical models to investigate the petrogenesis of modern-day deep mantle-derived rocks and (3) as a new series of normalising factors for mantle plume and intraplate lavas. The importance of presenting new mantle plume primary magma and reservoir compositions is highlighted in current geochemical databases (e.g., GEOROC: http://georoc.mpch-mainz.gwdg.de/georoc and EARTHREF: http://earthref.org/GERMRD) that contain standard compositions for many of Earth's mantle and crustal reservoirs [e.g., depleted MORB source mantle (DMM), HIMU, Enriched Mantle (EM), N-MORB, E-MORB], but not for mantle plume heads that generate large igneous provinces, and their deep mantle source regions.

2. Regional geology and sample collection

Curaçao is an island in the Netherlands Antilles and is located in the southern Caribbean Sea 70 km north of the coast of Venezuela (Fig. 1a). The geology of the island was first studied in detail by Beets (1972, 1977) who separated the strata into a ≥5 km thick, widespread late Cretaceous volcanic unit (the Curaçao Lava Formation: CLF), which is overlain by sedimentary rocks of the late Cretaceous and early Palaeogene (Danian) Knip Group and Middle Curaçao Formation respectively (Beets, 1972, 1977; Klaver, 1987; Kerr et al., 1996) (Fig. 1b). The base of the CLF is not exposed, but the lower sections are made up of pillow basalts and picrite lava flows (Klaver, 1987; Kerr et al., 1996). The middle of the CLF comprises pillow basalts and dolerite sills that give way to basaltic flows, sills and hyaloclastites in the upper sections (Klaver, 1987; Kerr et al., 1996). The late Cretaceous age and the detailed stratigraphy of the CLF are complex in detail and readers are referred to Loewen et al. (2013) for further information. Kerr et al. (1996), Hauff et al. (2000a) and Loewen et al. (2013) provide major and trace element and radiogenic isotope data to demonstrate that the CLF is derived from a mantle plume source region.

Twenty six picrites and basalts were collected from across the CLF as a terrestrial sampling project linked to the 2010 research cruise Meteor 81/2AB (IFM-GEOMAR, Germany) (Fig. 1b and Appendix A). Major element concentrations of the CLF lavas were determined using a JY Horiba Ultima 2 inductively coupled plasma optical emission spectrometer (ICP-OES) and the trace elements are analysed by a Thermo X series inductively coupled plasma mass spectrometer (ICP-MS) at Cardiff University, United Kingdom. A full description of all the analytical procedures and equipment at Cardiff University can be found in McDonald and Viljoen (2006). All sample data are presented in Tables A1 and A2 in Appendix A. Multiple analyses of international reference materials JB-1a and W2 were used to correct instrument drift and ensure the accuracy and precision of the analyses (see Table A3, Appendix A for standard data). Sr–Nd–Hf–Pb radiogenic isotope analyses were carried

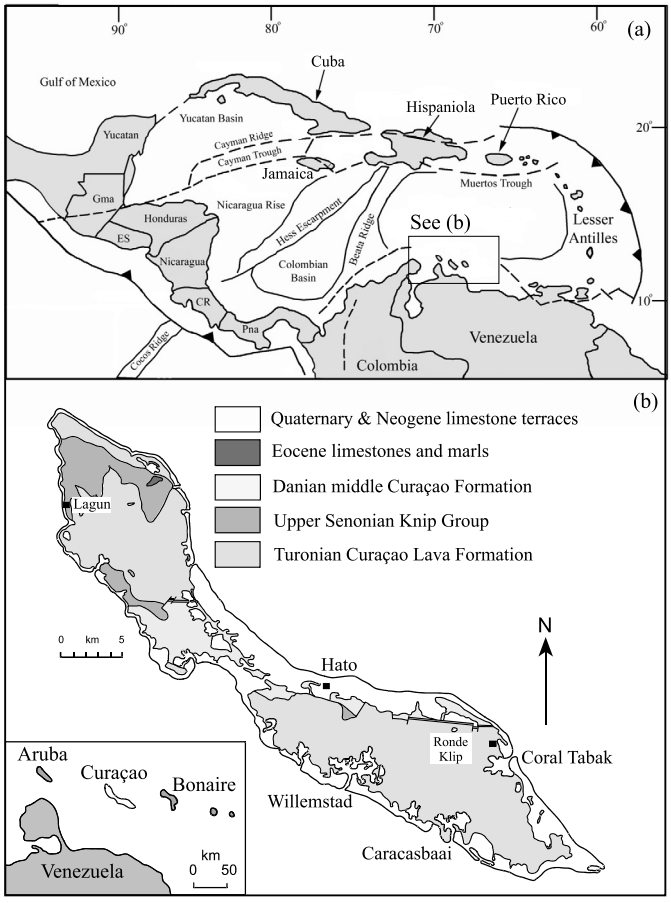

Fig. 1. (a) Map of the inter American region showing the location of the Netherlands Antilles and the island of Curaçao (boxed area). Gma, Guatemala; ES, El Salvador; CR, Costa Rica; Pma, Panama. (b) Simple geological map of Curaçao showing the location of the Curaçao Lava Formation. Exact location of samples can be found in Appendix A. Figure modified from Hastie and Kerr (2010).

out on six samples [$^{40}Ar/^{39}Ar$ ages and major and trace element data reported in Loewen et al. (2013) and Table A1, Appendix A] at GEOMAR Helmholtz Centre for Ocean Research Kiel by thermal ionisation mass spectrometry for Sr–Nd–Pb and by multicollector ICP-MS for Hf. All isotope data are presented in Table A4 and a full description of the analytical procedures and equipment used can be found in the table caption.

3. Assessing element mobility in the Curaçao samples

Previous studies on Caribbean Cretaceous igneous rocks have demonstrated that many of the large ion lithophile elements (LILE) are variably mobilised by low and high temperature alteration processes (e.g., Hauff et al., 2000a; Hastie et al., 2007, 2008, 2011; Neill et al., 2010; West et al., 2014). It is therefore important to assess the influence of element mobility on the composition of the Curaçao lavas. One of the best ways of evaluating element mobility uses a method first employed by Cann (1970), whereby a known immobile element is plotted on the abscissa of a variation diagram and other elements are plotted on the ordinate. If the rocks are co-genetic and both elements immobile and moderately-highly incompatible the data should form a linear trend with a high correlation coefficient (r).

Figs. 2a and 2b show that Ba and Rb display a large degree of scatter when plotted against Nb and have very low r values <0.2. In contrast, data for Zr and Th generate single linear trends with $r = 0.94$ (Figs. 2c and 2d), which are similar to Y = 0.9, Ta = 0.98, Hf = 0.94 and U = 0.94. Additionally, all of the rare earth elements

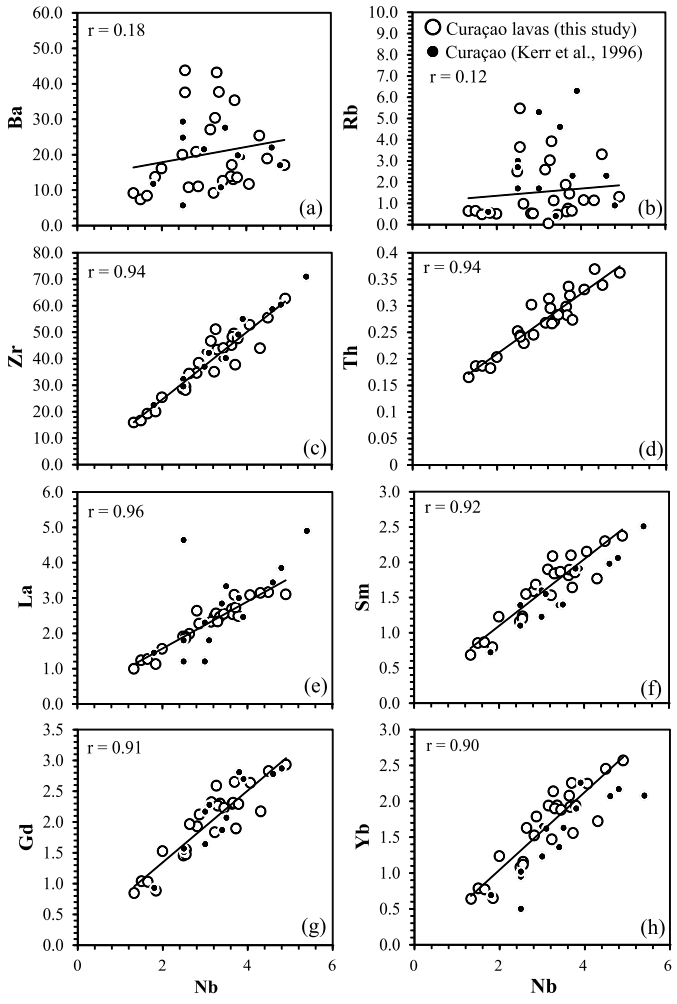

Fig. 2. (a–h) Representative LILE, HFSE and REE variation diagrams with Nb on the abscissa showing the possible mobilisation of elements during secondary alteration of the Curaçao lavas in this study. Previous Curaçao samples from Kerr et al. (1996) are also plotted. r = correlation coefficient for new data only.

(REE) form linear trends with high correlation coefficients which can be clearly seen in the La, Sm, Gd and Yb variation diagrams in Figs. 2e–h. These bivariate plots suggest that Ba and Rb (and other LILE) have been mobilised by low temperature alteration processes. Conversely, Th, U, the high field strength elements (HFSE) and the REE are immobile and confirm the previous proposal by Kerr et al. (1996) that the Curaçao lavas are co-genetic.

4. Classification of newly collected lavas

The Curaçao lavas have low SiO_2 contents $\leq$52 wt.% and can be broadly separated into a subgroup with moderate MgO contents from 7.20–11.31 wt.% and a subgroup with high MgO concentrations of 22.08–33.59 wt.% (Table A1, Appendix A). Combined Na_2O and K_2O contents are 0.13–3.93 wt.% and 0.13–1.39 wt.% for the two subgroups respectively. On total alkali silica (TAS), Zr/Ti–Nb/Y and Th–Co classification diagrams of Le Bas et al. (1992), Pearce (1996, after Winchester and Floyd, 1977) and Hastie et al. (2007) respectively the lavas with moderate MgO concentrations plot as tholeiitic basalts (Fig. 3a and b). The subgroup with high MgO contents have very high Co abundances (>75 ppm) and plot as basalts and picrobasalts on the TAS and Zr/Ti–Nb/Y diagrams (Fig. 3a). The extremely high MgO and Co suggests that the rocks have accumulated olivine. Rocks that plot in the basalt and picrobasalt fields on the TAS diagram that have no spinifex texture, SiO_2 <52 wt.%, MgO >12 wt.% and low alkali contents are classified as picrites (Le Bas, 2000; Kerr and Arndt, 2001) while the moderate MgO subgroup are tholeiitic basalts (Fig. 3a).

5. Fractional crystallisation and olivine accumulation

Curaçao major element variation diagrams show liquid lines of descent typical of basic lavas. Representative bivariate plots show that as MgO decreases SiO_2 increases and, initially, CaO and Al_2O_3 increase, but decrease at lower MgO contents (Fig. 3c–f). These trends have been explained by olivine fractional crystallisation and accumulation at MgO concentrations of >8–10 wt.% and olivine, clinopyroxene and plagioclase fractional crystallisation at lower MgO contents (Kerr et al., 1996; Trela et al., 2015). Similarly, below ~8–10 wt.% MgO plagioclase and clinopyroxene commonly crystallise together and cause the total Fe content (here reported as Fe_2O_3) of magmas to increase, which is evident by the negative trend at MgO <10 wt.% in Fig. 3f.

Problems can occur when calculating primary magma compositions for many primitive lavas because it is difficult to accurately correct for substantial fractional crystallisation of clinopyroxene and plagioclase (e.g., Korenaga and Kelemen, 2000; Herzberg and O'Hara, 2002). Therefore, it is advantageous to determine primary magma compositions from primitive lavas that have only crystallised or accumulated olivine on their ascent to the surface. PRIMELT3 software from Herzberg and Asimow (2015) is specifically designed to determine the composition of primary magmas from primitive lavas by successive additions or subtractions of equilibrium olivine. We use PRIMELT3 software here on COP and OJP primitive lavas that have only fractionated olivine. Previous results of using PRIMELT3 are similar to modelling in other recent studies (e.g., Coogan et al., 2014).

Oceanic plateau lavas, and basalts from other tectonic environments, commonly fractionally crystallise olivine + plagioclase + clinopyroxene and it is rare to find primitive lavas that have solely fractionated olivine on ascent (e.g., Kerr et al., 1996; Korenaga and Kelemen, 2000; Fitton and Godard, 2004; Hastie and Kerr, 2010; Loewen et al., 2013). Of the 26 lavas from Curaçao only 4 show compositional evidence (variation diagrams in Fig. 3 and PRIMELT3 computations) for exclusive olivine fractional crystallisation or accumulation. Despite alteration it is still possible to identify the phenocryst phases in thin section, even olivine. Most samples lack phenocryst phases and have an olivine, pyroxene and plagioclase groundmass that has been altered to several secondary minerals (e.g., clay minerals, chlorite and serpentine). Only 25 of the 76 OJP samples in Fitton and Godard (2004) show geochemical evidence for predominant olivine removal during ascent. This is confirmed by petrographic analysis whereby the 25 OJP samples contain only olivine phenocrysts in an aphanitic groundmass of olivine, clinopyroxene, plagioclase, Cr-spinel, titanomagnetite and sulphides. Plagioclase phenocrysts are occasionally seen, but only comprise $\ll$1 modal percent and therefore do not represent significant plagioclase fractionation. Fig. 4a is a primitive mantle normalised multielement diagram showing the composition of the primitive COP and OJP lavas that have only fractionated olivine.

6. Determining the composition of the Caribbean and Ontong Java primary magmas and their respective mantle plume source regions: methodologies and results

6.1. Major element composition of COP and OJP primary magmas

Using primitive lavas from the COP and OJP, the major element composition of primary magmas from both the Caribbean and Ontong Java large igneous provinces can be calculated using PRIMELT3 software. Full details on the successive develop-

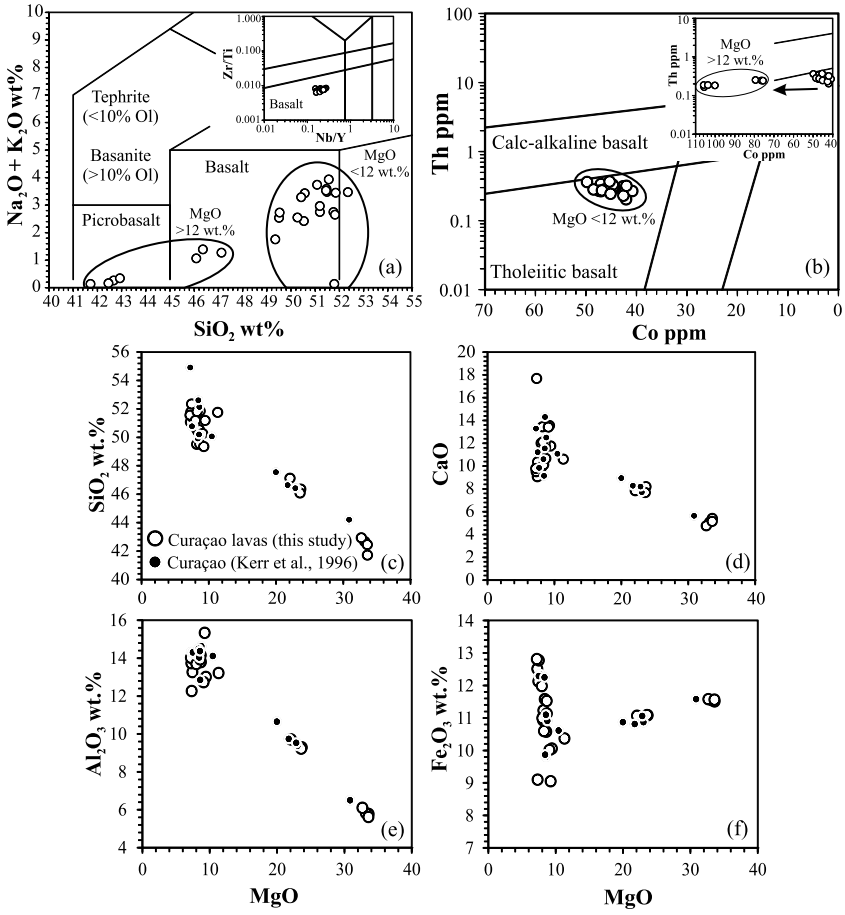

Fig. 3. (a) Total alkali silica (TAS) and Zr/Ti–Nb/Y plot from Le Bas et al. (1992) and Pearce (1996) [based on the original diagram from Winchester and Floyd, 1977]. (b) Th–Co classification diagram of Hastie et al. (2007). (c–f) Representative major element bivariate diagrams illustrating the liquid line of descent for the Curaçao lavas. Symbols as in Fig. 2.

ment of PRIMELT3 can be found in Herzberg and O'Hara (2002), Herzberg and Asimow (2008) and Herzberg and Asimow (2015). PRIMELT3 uses inverse and forward models to determine the major element composition of primary anhydrous melts. The inverse model involves calculating the array of possible primary magma compositions from a chosen primitive lava by the successive addition or subtraction of equilibrium olivine in 1 weight per cent increments. The forward model involves a peridotite source with a known composition and mineralogy being selected and experimental data and mass balance solutions are used to determine the compositions and melt fractions of derivative magmas at a range of conditions (temperatures, pressures, batch melting, fractional melting, etc.). The "primary magma array" in the inverse model is compared to the results of the forward model in projection (e.g., olivine–anorthite–quartz) and bivariate (e.g., FeO–MgO) diagrams. The composition of the *sought after primary melt* is determined by identifying the composition of the potential primary melt that has the same melt fraction in both bivariate and projection plots. In order to determine the major element composition of the primary magma of a primitive lava the software user is required to input (1) the major element composition of the primitive lava, (2) the estimated $Fe^{2+}/\Sigma Fe$ ratio and (3) the major element composition of the source peridotite from which the primary magma is to be derived.

Major element input parameters into the software include SiO_2, TiO_2, Al_2O_3, Cr_2O_3, FeO(t), MnO, MgO, CaO, Na_2O, K_2O, NiO and P_2O_5 in weight percent. With regards to the new Curaçao analyses in this paper, most samples are slightly hydrous due to secondary alteration and Fe is determined as $Fe_2O_3(t)$. Therefore, in order for the Curaçao (and OJP) lavas to be studied using PRIMELT3 the major elements have been normalised to anhydrous values, Ni and Cr trace element contents have been converted to wt.% oxide and added to the major elements and $Fe_2O_3(t)$ is converted to $FeO(t)$.

Modern analyses of both FeO and Fe_2O_3 in fresh lavas by titration is relatively rare for large igneous provinces, but data in Skovgaard et al. (2001) and models in Herzberg et al. (2007) show and assume respectively that oceanic plateau magmas have $Fe^{2+}/\Sigma Fe$ of ~0.9. We therefore use a value of 0.9 in all new COP and OJP computations in this study. The only exception to this is sample 10HK27 (Table A1, Appendix A) which produces a successful PRIMELT3 solution that requires olivine accumulation. Because this lava partly comprises cumulate olivine, which would have added Fe^{2+}, we have allowed PRIMELT3 to calculate the $Fe^{2+}/\Sigma Fe$ content of 10HK27 relative to a Fe_2O_3/TiO_2 ratio of 0.5 (see Herzberg and Asimow, 2008 for more information on this methodology).

Previously published major and trace element and radiogenic isotope concentrations for the COP and OJP lavas (e.g., Kerr et al., 1996; Hauff et al., 1997, 2000a, 2000b; Fitton and Godard, 2004; Hoernle et al., 2004; Hastie et al., 2008; Hastie and Kerr, 2010; Herzberg et al., 2007; Tejada et al., 2002, 2004) suggest that the mantle plume source regions of the COP and OJP are relatively fertile peridotites. Following Herzberg (2004) and Hastie and Kerr (2010), we take the major element composition of the fertile (pyrolitic) peridotite KR-4003 (Walter, 1998) to be representative of the COP and OJP mantle plume source regions. The major ele-

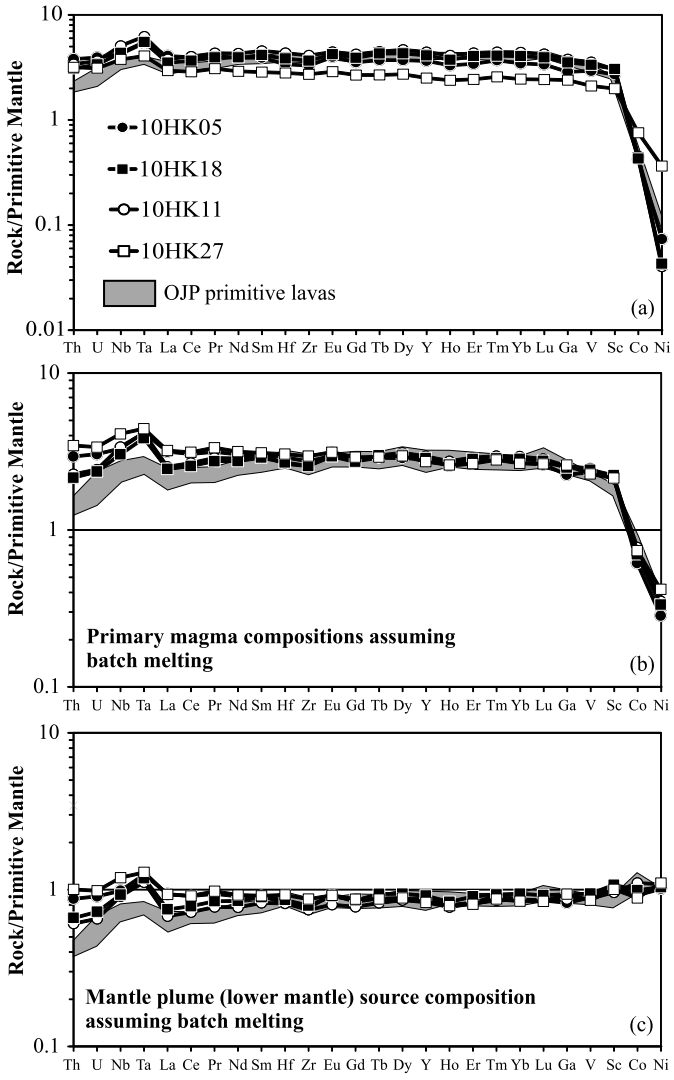

Fig. 4. (a) Primitive mantle normalised multielement diagrams showing the immobile trace element compositions of (a) the most primitive (only fractionated olivine) COP and OJP lavas, (b) COP and OJP primary magmas when derived by batch partial melting and (c) the composition of the COP and OJP mantle plume (lower mantle) source regions assuming batch melting. Normalising values from McDonough and Sun (1995). OJP samples 1183-5 and 1186-3 not included.

ment composition of KR-4003 is used as a presumed mantle plume source analogue with which to calculate primary magma major and trace element compositions and, subsequently, the trace element abundances of mantle plume sources. The major element composition of KR-4003 is very similar to the estimate for silicate Earth as proposed by McDonough and Sun (1995). Furthermore, both Allègre et al. (1995) and McDonough (2001) suggest that the whole mantle has a relatively homogeneous major element composition.

COP and OJP primary melt compositions generated by both batch and accumulated fractional melting are shown in Table 1 and Table A4, Appendix A. PRIMELT3 computations suggest that all of the primary melts are derived from final melting pressures as low as ~0.5–1 GPa. These shallow depths are consistent with relatively high Al_2O_3 contents at a given melt fraction in the computed primary magma compositions (e.g., Hirose and Kushiro, 1993; Walter, 1998). PRIMELT3 also determines (1) the weight percent olivine addition/subtraction required to generate the primary magma composition, (2) the olivine liquidus temperature, (3) the mantle potential temperature, (4) the olivine composition that co-

Table 1
Starting original primitive lava compositions and successful PRIMELT3 primary magma compositions for the Curaçao samples relative to batch and accumulated fractional melting (BM and FM respectively). Ol, wt.%, addition or subtraction of olivine required to generate the primary magma composition; Tol, olivine liquidus temperature; Tp, mantle potential temperature; Fo, olivine composition coexisting with the primary magma; F, fraction of partial melting required to generate the primary magma.

	SiO_2	TiO_2	Al_2O_3	Cr_2O_3	Fe_2O_3	FeO	MnO	MgO	CaO	Na_2O	K_2O	NiO	P_2O_5	Total	Ol wt.%	Tol	Tp	Kd	Fo	F
Original primitive lava composition																				
10HK05	51.997	0.860	13.217	0.070	1.021	8.273	0.163	9.576	11.954	2.726	0.068	0.019	0.056	100						
10HK11	49.850	1.007	14.204	0.052	1.131	9.160	0.184	8.240	13.543	2.428	0.126	0.010	0.064	100						
10HK18	51.364	0.932	14.167	0.052	1.075	8.709	0.170	8.740	12.262	2.357	0.105	0.011	0.058	100						
10HK27	46.309	0.602	9.286	0.289	0.301	9.692	0.173	23.636	8.193	1.321	0.067	0.091	0.039	100						
Primary magma composition with BM																				
10HK05	49.684	0.690	10.550	0.062	0.813	8.571	0.160	17.527	9.579	2.171	0.054	0.092	0.045	100	22.873	1396	1500	0.311	0.921	0.298
10HK11	47.189	0.728	10.190	0.043	0.808	9.500	0.178	19.624	9.768	1.736	0.090	0.099	0.045	100	33.744	1432	1554	0.301	0.924	0.269
10HK18	48.539	0.695	10.489	0.044	0.793	9.065	0.165	19.142	9.123	1.739	0.077	0.085	0.043	100	30.536	1421	1542	0.308	0.924	0.307
10HK27	46.717	0.648	10.005	0.304	0.325	9.941	0.178	21.443	8.823	1.426	0.073	0.075	0.043	100	−7.608	1459	1600	0.299	0.928	0.292
Primary magma composition with FM																				
10HK05	50.196	0.729	11.157	0.064	0.861	8.597	0.162	15.638	10.123	2.298	0.057	0.070	0.048	100	17.173	1362	1452	0.312	0.912	0.284
10HK11	47.569	0.770	10.802	0.045	0.858	9.603	0.182	17.759	10.349	1.842	0.096	0.078	0.048	100	27.788	1400	1506	0.303	0.916	0.255
10HK18	49.062	0.741	11.201	0.046	0.848	9.146	0.168	17.001	9.735	1.859	0.083	0.064	0.045	100	23.830	1385	1487	0.310	0.914	0.291
10HK27	47.117	0.692	10.692	0.318	0.347	10.117	0.182	19.401	9.424	1.526	0.078	0.060	0.046	100	−14.334	1426	1548	0.302	0.919	0.294

Table 2
Primary magma trace element compositions for the COP with regards to batch melting. The *D*-values used to calculate the primary magmas are discussed in Appendix A. Trace elements in ppm. Nickel values are calculated using equation (4).

	Original composition				Primary magma composition with batch melting			
Sample	10HK05	10HK11	10HK18	10HK27	10HK05	10HK11	10HK18	10HK27
F (*X* for 10HK27)					0.771	0.663	0.695	0.076
Sc	44.0	49.0	49.5	32.3	35.1	34.3	36.0	34.6
V	241.0	292.2	274.6	173.1	190.6	201.5	197.6	186.0
Co	44.6	47.5	45.1	79.4	64.5	81.1	73.2	77.3
Ni	144	79	84	715	555	686	654	819
Ga	11.503	15.140	14.122	9.586	8.965	10.198	9.954	10.344
Y	15.710	19.080	17.690	10.800	12.120	12.647	12.293	11.689
Zr	34.613	43.265	38.503	28.610	26.697	28.667	26.747	30.966
Nb	2.810	3.349	2.861	2.484	2.168	2.219	1.988	2.688
La	2.641	2.464	2.275	1.914	2.037	1.633	1.580	2.071
Ce	6.609	6.734	6.144	4.825	5.097	4.462	4.268	5.222
Pr	1.033	1.100	1.000	0.782	0.797	0.729	0.695	0.847
Nd	4.891	5.376	4.929	3.635	3.772	3.562	3.424	3.934
Sm	1.591	1.849	1.684	1.160	1.227	1.225	1.170	1.256
Eu	0.614	0.686	0.650	0.444	0.474	0.454	0.452	0.481
Gd	1.929	2.301	2.124	1.458	1.488	1.525	1.476	1.578
Tb	0.369	0.444	0.424	0.266	0.285	0.294	0.295	0.287
Dy	2.500	3.147	2.900	1.840	1.929	2.085	2.015	1.992
Ho	0.494	0.614	0.558	0.356	0.381	0.407	0.388	0.386
Er	1.501	1.906	1.776	1.068	1.158	1.264	1.235	1.155
Tm	0.252	0.302	0.278	0.175	0.194	0.200	0.194	0.190
Yb	1.525	1.942	1.789	1.081	1.179	1.292	1.247	1.169
Lu	0.228	0.287	0.266	0.164	0.176	0.191	0.185	0.177
Hf	0.962	1.230	1.088	0.794	0.745	0.819	0.760	0.859
Ta	0.200	0.231	0.204	0.151	0.154	0.153	0.142	0.163
Th	0.302	0.271	0.246	0.253	0.233	0.179	0.171	0.273
U	0.080	0.074	0.069	0.063	0.062	0.049	0.048	0.068

exists with the primary magma and (5) the fraction of partial melting needed to generate the primary melt (Table 1 and Table A4 in Appendix A). The 29 samples from the COP and OJP generate primary magmas with high CaO contents at a given MgO abundance and have internally consistent major element systematics to rule out a pyroxenite source region (see Herzberg and Asimow, 2008 for more information). Finally, the successful COP and OJP primary melts computed with PRIMELT3 have high SiO_2 abundances relative to a given CaO content which rule out the involvement of a volatile-rich peridotite source region (again, see Herzberg and Asimow, 2008 for further information on this filter).

6.2. Calculating the trace element composition of the COP and OJP primary magmas

PRIMELT3 only calculates the major element composition of the primary COP and OJP magmas (Table 1 and Table A4, Appendix A). In order to determine the trace element concentrations of the COP and OJP primary magmas we have to correct for olivine fractional crystallisation or accumulation in the primitive lavas. If we take the results assuming that the primitive lavas are derived from batch melting we can use the (Rayleigh) fractional crystallisation equation to add the relevant percentage of olivine back into the primitive lava to obtain the primary magma compositions. All but one of the COP and OJP primitive lavas has lost olivine via fractional crystallisation and the equation used to correct for this is:

$$C_0 = \frac{C_l}{F^{(D_{ol}-1)}} \tag{1}$$

where C_0 is the initial concentration of an element prior to olivine fractionation (the primary magma composition), C_l is the concentration of the element in the primitive lava in question, F is the proportion of melt remaining and D_{ol} is the partition coefficient of fractionating olivine (see Appendix A for information on the choice of D_{ol} values). F values are derived from the PRIMELT3 computations. Sample 10HK27 is different as it has accumulated olivine and, as such, a set mass fraction of olivine has to be removed from the primitive lava to give the primary magma composition. We calculate the removal using the mass balance equation:

$$C_0 = \frac{C_l - (XC_{ol})}{1 - X} \tag{2}$$

where definitions are as before except X is the mass fraction of olivine that has accumulated in 10HK27 (Table 2) and C_{ol} is the concentration in the olivine being removed that we estimate by using the equation:

$$C_{ol} = D_{ol}C_l \tag{3}$$

Correcting NiO for olivine fractionation or accumulation is difficult because the Ni D_{ol} value is extremely sensitive to melt composition, temperature and pressure variations (e.g., Trela et al., 2015). Additionally, Herzberg and Asimow (2015) show that NiO contents derived from PRIMELT3 can be too high if primitive lavas are derived from mixing of primary magmas with olivine-fractionated derivative melts. Therefore, although the NiO contents in Table 1 and Table A4 are the values originally computed by PRIMELT3, we determine the Ni concentrations in the primary magmas and mantle plume source regions by treating Ni as a trace element. Accordingly we calculate the Ni content of the primary magmas using the equation:

$$\text{Ni ppm} = 21.6\text{MgO} - 0.32\text{MgO}_2 + 0.051\text{MgO}_3 \tag{4}$$

It is an important step to use equation (4) (see Herzberg and Asimow, 2015 for derivation) because it was found in the course of this study that the PRIMELT3 NiO values are too high in the primary magmas and if not corrected can translate into extremely high NiO values in the mantle plume source regions relative to elements with similar incompatibilities.

The results of all of these calculations are shown in a representative primitive mantle normalised diagram in Fig. 4b and the data can be found in Table 2 and Table A5 in Appendix A to illustrate the full trace element contents of the COP and OJP mantle plume-derived primary magmas.

Table 3
Composition of COP mantle plume (lower mantle) source region with regards to batch melting. The *D*-values used to calculate the source are discussed in Appendix A. Trace elements in ppm. Nickel values are determined using data in Table 2 that are derived from equation (4).

	Composition of COP source prior to batch melting			
Sample	10HK05	10HK11	10HK18	10HK27
F	0.298	0.269	0.307	0.292
Sc	16.7	15.6	17.4	16.3
V	73.1	72.1	77.4	70.3
Co	97.0	116.0	104.2	93.1
Ni	1982	2124	2033	2163
Ga	3.300	3.483	3.744	3.747
Y	3.778	3.576	3.940	3.569
Zr	8.059	7.812	8.312	9.147
Nb	0.648	0.598	0.612	0.786
La	0.608	0.439	0.486	0.605
Ce	1.525	1.203	1.315	1.528
Pr	0.239	0.197	0.214	0.248
Nd	1.134	0.966	1.060	1.157
Sm	0.371	0.334	0.364	0.371
Eu	0.143	0.124	0.140	0.142
Gd	0.456	0.423	0.465	0.474
Tb	0.087	0.082	0.093	0.086
Dy	0.591	0.578	0.635	0.598
Ho	0.119	0.115	0.124	0.118
Er	0.362	0.358	0.397	0.354
Tm	0.062	0.058	0.063	0.059
Yb	0.383	0.383	0.416	0.372
Lu	0.058	0.057	0.062	0.057
Hf	0.232	0.231	0.243	0.262
Ta	0.046	0.041	0.044	0.048
Th	0.070	0.048	0.052	0.080
U	0.018	0.013	0.015	0.020

6.3. Calculating the trace element composition of the COP and OJP mantle plume source regions

The calculated COP and OJP primary magma trace element concentrations have been used to determine the composition of the mantle plume sources. PRIMELT3 computes melt fractions (F) for batch and accumulated fractional melting of a fertile peridotite., Here we use the batch melting equation from Shaw (1970) to calculate the composition of the mantle plume sources. The actual melting process in a mantle plume will be somewhere between fractional and batch melting, but is unlikely to be close to perfect fractional melting at the melt fractions estimated here. In any case, large-degree fractional melting effectively strips the residual mantle of all incompatible elements, and so their concentration in the un-melted mantle source can easily be calculated by mass balance and will be equal to $C_l F$. Given that the large degrees of melting estimated here will result in a harzburgite residue and that all incompatible elements will have $D_{ol} \approx D_{opx} \approx 0$, the original mantle source composition calculated by assuming either fractional or batch melting will be virtually identical. If we know the value of F and the modal proportion of phases in the residue after melting, it is straightforward to calculate the un-melted source composition by mass balance.

$$C_0 = C_l F + C_r(1 - F) \quad (5)$$

and

$$C_r = D C_l \quad (6)$$

where C_0, C_l and C_r are the concentrations of an element in, respectively, the un-melted mantle source, the liquid produced by partial melting, and the residual mantle. D is the bulk distribution coefficient for the residual phases. By combining (5) and (6) we obtain:

$$C_0 = C_l\big(F + D(1 - F)\big) \quad (7)$$

which is Shaw's (1970) modal batch melting equation. The mass balance parameterisation of Herzberg and O'Hara (2002), partial melt experiments on KR-4003 by Walter (1998) and several other experimentally derived mineral and melt modes for various peridotite starting compositions (e.g., Gudfinnsson and Presnall, 1996; Kinzler, 1997; Johnson, 1998) show that for ~27–31% melting at 1.5–4.0 GPa there will be ~75 wt.% olivine and ~25 wt.% orthopyroxene in the residual mantle. Therefore, D values have been calculated using modal fractions of 0.75 olivine and 0.25 orthopyroxene (see Appendix A for the choice of D values).

There is no need to use the non-modal melting equations and successively remove phases as melting progresses because, at >25% melting, garnet or spinel and clinopyroxene would have been exhausted and the liquid would be in equilibrium with only olivine and orthopyroxene and sit on a cotectic between these phases. Consequently, we do not need to know the proportion of phases in the un-melted mantle source, the modal melting proportions, or the D values for garnet, spinel and clinopyroxene. Our calculations require only that we know the melt fraction and the proportion of phases in the residual mantle. Appendix B is a simple excel spreadsheet that gives a worked example and shows that Shaw's (1970) modal and non-modal melting equations give identical results when D is calculated from the residual assemblage. The computed trace element composition of COP and OJP source regions are shown in Fig. 4c and Table 3 and Table A6 in Appendix A.

7. Discussion

7.1. Compositionally different mantle plumes and comparison to other mantle and crustal reservoirs

The calculations indicate that the COP and OJP primary magmas have identical M-HREE, Zr, Hf and Y abundances (Fig. 4b, Table 2 and Table A5). Conversely, the most incompatible elements (Th, U, Nb, Ta and the LREE) are more enriched in the COP primary magmas than in the OJP melts. The incompatible trace element-enriched nature of the COP samples is replicated when the compositions of the source regions are calculated (Figs. 4c and 5a and Table 3 and Table A6 in Appendix A). When normalised to primitive mantle both the COP and OJP source regions again have similar M-HREE, Zr, Hf and Y concentrations. Nevertheless, Figs. 4c and 5 demonstrate that the COP mantle plume source region is more enriched in Th, U, Nb, Ta and the LREE than the OJP mantle plume.

Representative $\varepsilon Nd_{120\,Ma}$–$\varepsilon Hf_{120\,Ma}$ and $(^{206}Pb/^{204}Pb)_{120\,Ma}$–$(^{207}Pb/^{204}Pb)_{120\,Ma}$ diagrams are shown in Fig. 5c and d. The Curaçao lavas range from 92–62 Ma (Loewen et al., 2013), but we have corrected the initial Curaçao radiogenic isotopes from this study and the literature to 120 Ma using the average calculated source parent/daughter ratios (Table A4) so that they can be compared with the OJP isotopic composition. Although there is considerable overlap between the COP and OJP in $\varepsilon Hf_{120\,Ma}$ and $\varepsilon Nd_{120\,Ma}$, the COP extends to more depleted compositions (Fig. 5c). In contrast, there is no overlap in Pb isotopic composition on the uranogenic Pb isotope diagram at 120 Ma and the COP has more enriched Pb isotope ratios (Fig. 5d). More depleted Nd and Hf yet more enriched Pb isotopic compositions for the COP indicate that the COP source cannot simply be related to the OJP source by greater time-integrated incompatible element enrichment of the COP source. In summary, the incompatible element and isotope data show that the two oceanic plateaus are derived from distinct source material, despite similarity in the major element composition of their sources.

Fig. 5 and Table 4 compare the COP and OJP source regions with representative crustal and mantle reservoirs commonly used in

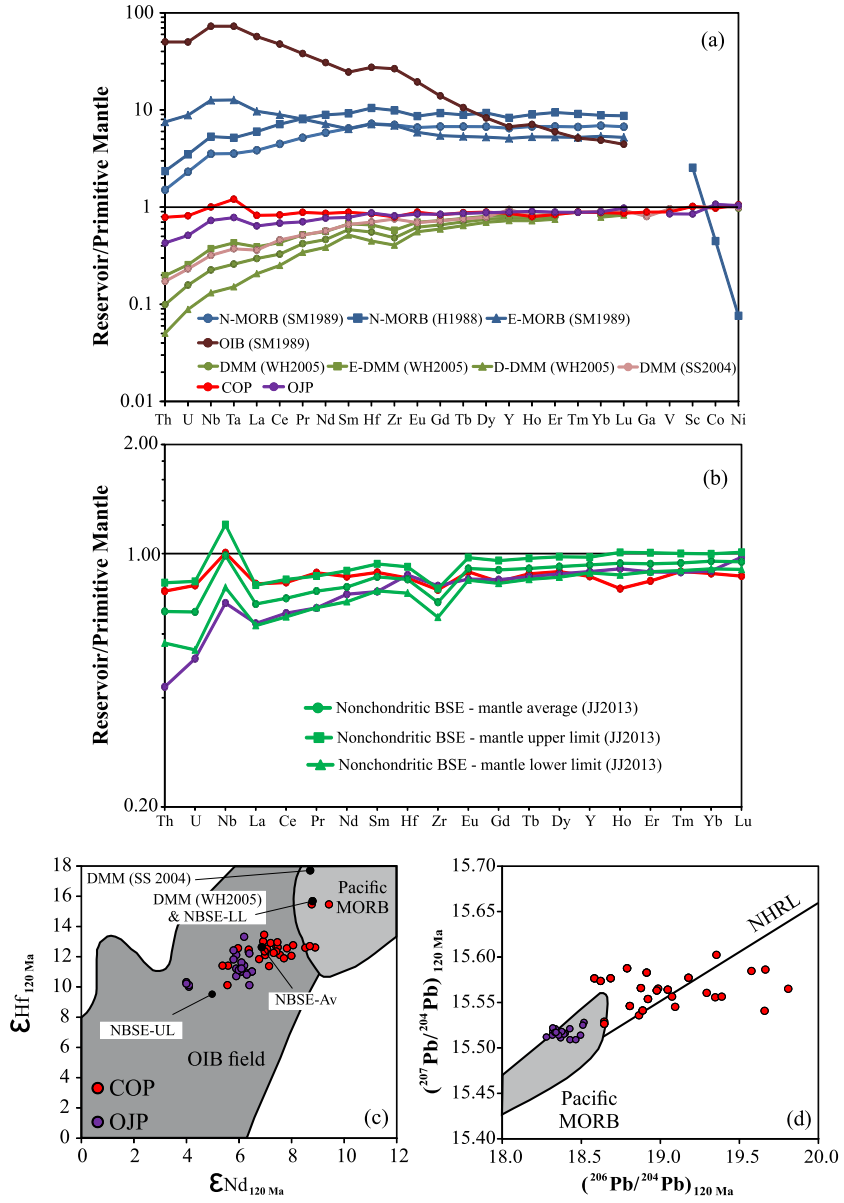

Fig. 5. (a) Primitive mantle normalised multielement diagram comparing the average COP and OJP mantle source compositions with representative crustal and mantle reservoirs commonly used in previous geochemical modelling. Reference abbreviations same as Table 4. (b) Primitive mantle normalised diagram showing the lower mantle source compositions in this study relative to the recent trace element estimates for non-chondritic bulk silicate Earth (BSE) from Jackson and Jellinek (2013) (JJ2013). Primitive mantle normalising values from McDonough and Sun (1995). OJP samples 1183-5 and 1186-3 not included in OJP average. (c) $\varepsilon Nd_{120\,Ma}$–$\varepsilon Hf_{120\,Ma}$ diagram showing the more radiogenic COP rocks relative to the OJP samples based on Nd isotope ratios. OIB and MORB fields from Geldmacher et al. (2003) and Tejada et al. (2004). DMM and NBSE data from references cited in Table 4. (b) $(^{206}Pb/^{204}Pb)_{120\,Ma}$–$(^{207}Pb/^{204}Pb)_{120\,Ma}$ plot showing that, compared to the OJP, samples from the COP are, again, more radiogenic. MORB field and Northern Hemisphere Reference Line from Hauff et al. (2000a, 2000b) and Tejada et al. (2004). COP data are from this study, Kerr et al. (1996), Hauff et al. (2000a, 2000b), Geldmacher et al. (2003), Thompson et al. (2003) and Hastie et al. (2008). OJP data are from Tejada et al. (2004). COP and OJP data are age corrected to 120 Ma so that they can be compared to one another, but it should be noted that the COP is considered to be ≤90 Ma.

geochemical modelling. Relative to the several DMM source compositions from Salters and Stracke (2004) and Workman and Hart (2005), the new mantle plume source compositions calculated in this paper are generally more enriched in all the more incompatible elements, which becomes pronounced with elements more incompatible than the MREE. Relative to chondritic primitive mantle values (Hofmann, 1988 and McDonough and Sun, 1995), the mantle plume source compositions are slightly depleted in nearly all the trace elements with the OJP source being more depleted compared with the COP source. A notable exception to this is that the COP source has slightly enriched Nb and Ta concentrations relative to chondritic primitive mantle. This feature also highlights the fact that, similar to the E-DMM, E-MORB and OIB reservoirs, both the COP and OJP mantle plume source regions have positive Nb and Ta anomalies (Fig. 5a and Table 4).

The exact process by which Nb and Ta become enriched in mantle sources relative to other trace elements with similar compatibilities is debated. However, previous hypotheses have explained the relative enrichment as a result of *minor* amounts of rutile-bearing recycled oceanic crust (eclogite) in the mantle source region or variable trace element partitioning between phases in the deep mantle (e.g., Hofmann and White, 1982; Fitton et al., 1997; Fitton, 2007; Jackson et al., 2008; Trela et al., 2015). Relative to the OJP source, a larger amount of a rutile-bearing recycled oceanic crust component in the source of COP would not only explain the higher Th, U, Nb, Ta and LREE abundances in

Table 4
Trace element comparison of representative crustal and mantle reservoirs commonly used in geochemical models. Res., crustal or mantle reservoir; Ref., reference; SM(1989), Sun and McDonough (1989); H(1988), Hofmann (1988); WH(2005), Workman and Hart (2005); SS(2004), Salters and Stracke (2004); MS(1995), McDonough and Sun (1995); JJ(2013), Jackson and Jellinek (2013); NBSE, non-chondritic BSE; Av, average; UL, upper limit; LL, lower limit. Trace elements in ppm. OJP average does not include samples 1183-5 and 1186-3.

Res. Ref.	N-MORB SM(1989)	N-MORB H(1988)	E-MORB SM(1989)	OIB SM(1989)	DMM WH(2005)	E-DMM WH(2005)	D-DMM WH(2005)	DMM SS(2004)	PM H(1988)	PM MS(1995)	NBSE-Av JJ(2013)	NBSE-UL JJ(2013)	NBSE-LL JJ(2013)	COP	OJP
Th	0.12	0.1871	0.6	4	0.0079	0.0157	0.004	0.0137	0.0813	0.0795	0.055	0.066	0.045	0.063	0.034
U	0.047	0.0711	0.18	1.02	0.0032	0.0052	0.0018	0.0047	0.0203	0.0203	0.014	0.017	0.011	0.017	0.010
Nb	2.33	3.507	8.3	48	0.1485	0.2462	0.0864	0.21	0.6175	0.658	0.65	0.79	0.53	0.661	0.480
Ta	0.132	0.192	0.47	2.7	0.0096	0.0159	0.0056	0.0138	0.0351	0.037				0.045	0.029
La	2.5	3.895	6.3	37	0.192	0.253	0.134	0.234	0.6139	0.648	0.47	0.53	0.41	0.534	0.416
Ce	7.5	12.001	15	80	0.55	0.726	0.421	0.772	1.6011	1.675	1.26	1.42	1.12	1.393	1.146
Pr	1.32	2.074	2.05	9.7	0.107	0.132	0.087	0.131	0.2419	0.254	0.2	0.22	0.18	0.225	0.180
Nd	7.3	11.179	9	38.5	0.581	0.703	0.483	0.713	1.1892	1.25	1.01	1.12	0.92	1.079	0.965
Sm	2.63	3.752	2.6	10	0.239	0.273	0.21	0.27	0.3865	0.406	0.35	0.38	0.32	0.360	0.319
Hf	2.05	2.974	2.03	7.8	0.157	0.186	0.127	0.199	0.2676	0.283	0.24	0.26	0.22	0.242	0.247
Zr	74	104.24	73	280	5.082	6.087	4.269	7.94	9.714	10.5	7.7	8.4	7	8.333	8.551
Eu	1.02	1.335	0.91	3	0.096	0.108	0.086	0.107	0.1456	0.154	0.14	0.15	0.13	0.137	0.131
Gd	3.68	5.077	2.97	7.62	0.358	0.397	0.324	0.395	0.5128	0.544	0.49	0.52	0.45	0.455	0.460
Tb	0.67	0.885	0.53	1.05	0.07	0.076	0.064	0.075	0.094	0.099	0.09	0.096	0.084	0.087	0.085
Dy	4.55	6.304	3.55	5.6	0.505	0.543	0.471	0.531	0.6378	0.674	0.62	0.66	0.58	0.601	0.592
Y	28	35.82	22	29	3.328	3.548	3.129	4.07	3.94	4.3	4	4.2	3.8	3.716	3.832
Ho	1.01	1.342	0.79	1.06	0.115	0.123	0.108	0.122	0.1423	0.149	0.14	0.15	0.13	0.119	0.135
Er	2.97	4.143	2.31	2.62	0.348	0.369	0.329	0.371	0.4167	0.438	0.41	0.44	0.39	0.368	0.390
Tm	0.456	0.621	0.356	0.35				0.06	0.0643	0.068	0.064	0.068	0.061	0.061	0.060
Yb	3.05	3.9	2.37	2.16	0.365	0.382	0.348	0.401	0.4144	0.441	0.42	0.44	0.4	0.388	0.395
Lu	0.455	0.589	0.354	0.3	0.058	0.06	0.056	0.063	0.0637	0.0675	0.064	0.068	0.061	0.058	0.066
Ga								3.2		4				3.569	
V								79		82				73.2	70.0
Sc		41.37						16.3	14.88	16.2				16.5	13.8
Co		47.07						106	104	105				102.5	112.4
Ni		149.5			1909			1960	2080	1960				2076	2040

the COP data, but it also explains the more radiogenic Nd and Pb isotope systematics in Fig. 5c and d (e.g., Hauff et al., 2000a; Hastie et al., 2008; Trela et al., 2015).

7.2. Do the compositions of the mantle plume source regions tell us anything about the Earth's deep mantle?

Numerous studies (e.g., Kerr et al., 1995, 1996; Hauff et al., 2000a; Kempton et al., 2000; Hoernle et al., 2002, 2004; Geldmacher et al., 2003; Fitton and Godard, 2004; Herzberg, 2004; Tejada et al., 2002, 2004; Fitton, 2007; Hastie et al., 2008; Herzberg and Asimow, 2008; Hastie and Kerr, 2010) and the results of our calculations have highlighted the heterogeneous compositions in oceanic plateau-derived tholeiitic lavas generated from very high degrees of partial melting (up to ~30%) that have not been contaminated with continental crust. The high degrees of fusion required to generate oceanic plateau tholeiitic primary magmas mean that differing degrees of partial melting cannot explain the heterogeneous trace element and radiogenic isotope compositions in individual oceanic plateaus or the variation between different oceanic plateaus (e.g., COP, OJP or Iceland: Hauff et al., 2000a; Kempton et al., 2000; Tejada et al., 2004; Kokfelt et al., 2006; Fitton, 2007; Hastie et al., 2008; Kerr, 2014). Consequently, the chemical and isotopic heterogeneity of the COP, OJP and Iceland is related to their compositionally heterogeneous source regions, most likely reflecting differing amounts of recycled components added to a depleted lower mantle matrix(ices).

In order to assess if the compositions of the different COP and OJP mantle plume source regions in this study tell us anything about the Earth's deep mantle we first need to know: (1) if the COP and OJP mantle plume source regions represent the very deep mantle (e.g., potentially down to the core–mantle boundary: Campbell, 2007; French and Romanowicz, 2015) or shallow/lithospheric mantle sources? (e.g., Workman et al., 2004; Pilet et al., 2011) and (2) if the mantle plume sources are derived from the deep mantle, are they contaminated with large volumes of the upper mantle or lithospheric mantle?

The COP and OJP have estimated volumes of 35×10^6 km^3 and 60×10^6 km^3 respectively (Schubert and Sandwell, 1989; Coffin and Eldholm, 1994) and have been derived from mantle source regions by large degrees of partial melting (Fitton and Godard, 2004; Hastie and Kerr, 2010). Derivation of the COP and OJP by ~30% partial melting requires a source volume of the mantle more than 3 times the volume of the plateaus, which is much larger than any lithospheric source (Coffin and Eldholm, 1994). The volume of the upper mantle DMM reservoir is controversial, but may be theoretically large enough to supply the large volumes of magma required to generate an oceanic plateau (Workman and Hart, 2005; Boyet and Carlson, 2006; Caro and Bourdon, 2010). However, 30% partial melting calculations using DMM, D-DMM or E-DMM as source regions do not generate melts with compositions similar to primary magmas from the COP and OJP. Radiogenic isotope systematics also show that oceanic plateau lavas are distinct relative to MORB lavas (Fig. 5c and d) (e.g., Kerr et al., 1995; Hauff et al., 2000a; Kempton et al., 2000; Geldmacher et al., 2003; Hoernle et al., 2004; Tejada et al., 2004; Hastie et al., 2008; Jackson et al., 2015). Therefore, it is reasonable to assume that the source regions for the COP and OJP magmas are best represented by more enriched deeper mantle below the DMM reservoir.

Several geochemical and computational modelling studies suggest that ascending mantle plumes are not contaminated with upper mantle and even if they did entrain upper mantle it would not be heated enough by thermal conduction to allow it to undergo partial melting (e.g., Hart et al., 1992; Hauri et al., 1994; Kerr et al., 1995; Kempton et al., 2000; Farnetani et al., 2002; Tejada et al., 2002; Farnetani and Samuel, 2005; Fitton, 2007; Lohmann et al., 2009). Therefore, the geochemical signatures derived from our calculations of mantle plume source regions are unlikely to represent the source region for MORB (DMM) or a mixture between lower and upper mantle. Instead, we propose that the calculated source regions in this study represent portions of the deep mantle. We note that this may not hold true for other oceanic plateaus such as Iceland or modern hotspots such as Galápagos that show evidence of ridge interactions (e.g., Trela et al., 2015).

7.3. Similarity to a non-chondritic Earth?

Mantle plume-derived rocks that have the highest ^{3}He/^{4}He ratios and U/Pb ratios undisturbed for ~4.5 billion years are found on Baffin Island and West Greenland (Graham et al., 1998; Stuart et al., 2003; Starkey et al., 2012). It is suggested that high ^{3}He/^{4}He ratios in these lavas are derived from primitive un-degassed deep mantle source regions (e.g., Jackson et al., 2010). The Baffin Island and West Greenland lavas also have super-chondritic Nd and Hf isotope ratios (including ^{142}Nd/^{144}Nd) which suggest that although the mantle source region may have been primitive it either has to (1) represent non-chondritic material that accreted to form the early Earth or (2) the mantle source had to have undergone a period of melt extraction just after planetary formation (leading to depletion of an initial chondritic source) (e.g., Boyet and Carlson, 2006; Caro and Bourdon, 2010; Jackson et al., 2010). If it was the latter, the early depleted mantle reservoir has been interpreted as precursor of all other mantle reservoirs and is termed the non-chondritic bulk silicate Earth (BSE) composition (Jackson and Jellinek, 2013). Jackson and Jellinek (2013) used isotopically constrained parent–daughter ratios and canonical trace element ratios to determine the trace element composition of the present-day non-chondritic BSE reservoir that should represent a lower mantle reservoir. Interestingly, the composition of the COP and OJP deep mantle source regions (also with super-chondritic Nd and Hf radiogenic isotope ratios, Hauff et al., 2000a; Geldmacher et al., 2003; Tejada et al., 2004; Hastie et al., 2008; Jackson and Carlson, 2011) are very similar to the non-chondritic Earth compositions in Jackson and Jellinek (2013) (Fig. 5b and c). Consequently, the Caribbean and Ontong Java LIPs could potentially be derived from the most primitive mantle reservoir in the Earth's deep mantle.

7.4. Mantle heterogeneity and concluding remarks

The depleted MORB source reservoir supplies N-MORB magmas to form the oceanic crust and also contains enriched veins, blobs and/or streaks of recycled oceanic lithosphere that undergo small degrees of partial melting to form E-MORB and OIB magmas (e.g., Phipps Morgan and Morgan, 1999; Salters and Strake, 2004; Ito and Mahoney, 2005; Workman and Hart, 2005; Fitton, 2007). In Fig. 6 we show that the upper mantle reservoir extends down to the 660 km discontinuity. However, because of numerous variables in mantle–crust mass balance models, the size of the DMM in Fig. 6 is purely illustrative.

Similar to others in the literature (e.g., Phipps Morgan and Morgan, 1999), we argue that the mantle below the depleted upper mantle reservoir also contains small variably enriched areas (veins, blobs and/or streaks of recycled oceanic lithosphere) that become incorporated into mantle plumes and, after the ascent of the plume to the base of the lithosphere, undergo low degrees of partial melting (<5%) to form trace element and isotopically variable OIB lavas (source of the HIMU, EM1, EM2 or FOZO end-members, e.g., Hofmann and White, 1982; Zindler and Hart, 1986; Hart et al., 1992; Phipps Morgan and Morgan, 1999; Fitton, 2007; Herzberg and Gazel, 2009; Trela et al., 2015). These lower mantle enriched veins, blobs and/or streaks pond at the core–mantle

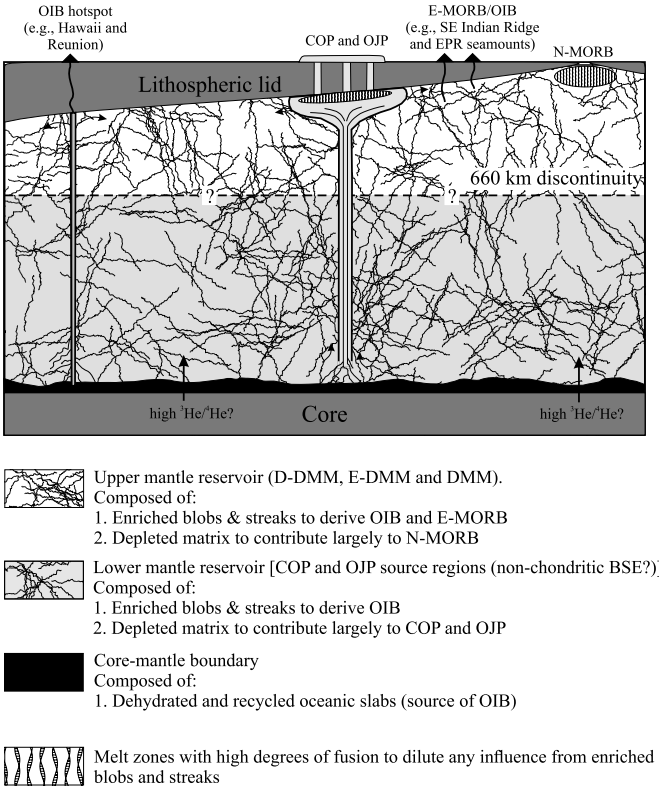

Fig. 6. Schematic diagram illustrating the broad compositional make up of the Earth's mantle. The lithospheric lid is represented by oceanic lithosphere only. Cross section is schematic and is not to scale. In reality the large mantle head should be located closer to the mid-ocean ridge.

boundary (as the residue of subducted slabs, e.g., Hofmann and White, 1982) or are dispersed in a depleted lower mantle peridotite matrix (e.g., Phipps Morgan and Morgan, 1999; Fitton, 2007). Trace element systematics suggest that the lower mantle matrix is relatively more enriched than the depleted peridotite matrix that makes up the bulk of the upper mantle reservoir (see Fitton, 2007 for a review).

Fig. 6 shows the theoretical lower mantle extending from the base of the MORB source reservoir to the core–mantle boundary. Plume tails (e.g., Hawaii and Réunion) undergo low degrees of partial melting beneath the lithosphere, especially thicker, older lithosphere, to preferentially sample the more fusible ascending enriched veins, blobs and/or streaks. Conversely, large plume heads that are composed of the entrained lower mantle matrix and enriched veins, blobs and/or streaks undergo high degrees of partial melting to give rise, for example, to the Caribbean, Ontong Java and Iceland large igneous provinces (Fig. 6). Most of the geochemical signature of the oceanic plateau primary melts is derived from the lower mantle matrix; however, high Th, U, LREE concentrations, positive Nb–Ta anomalies and radiogenic Nd and Pb radiogenic isotopes in the COP and OJP source regions are evidence of the small enriched areas (rutile-bearing recycled oceanic crust).

In conclusion, the Earth's mantle from the lithosphere to the core has a highly complex "marble cake" structure with numerous small variably enriched veins, blobs and streaks within much larger subtly enriched and depleted mantle matrices (e.g., Phipps Morgan and Morgan, 1999; Fitton, 2007). The task of locating (or mapping) small geographically distinct geochemical endmember reservoirs in the mantle using trace element and isotopic systematics may be a forlorn hope, because the mantle could be far too heterogeneous on a micro to macro scale. However, the two new mantle plume magma compositions calculated in this paper are generated by such high melt fractions that any influence from small geochemically distinct enriched zones in the resultant mantle plume primary magmas are diluted. Therefore, as with studying shallow mantle-derived lavas using the D-DMM, E-DMM and DMM reservoirs, the subtly enriched and depleted COP and OJP lower mantle source compositions in this paper can be used as distinct compositional entities to study the petrogenesis of mantle-derived rocks at the Earth's surface that have been derived from the deepest mantle.

Author contributions

A.R.H. conceived of the idea, wrote most of the paper, undertook most of the modelling and performed major and trace element preparation. J.G.F. co-wrote the paper, aided with the modelling and supplied data from the OJP. A.C.K. co-wrote the paper, supplied locality maps for Curaçao and aided the modelling. I.M. performed major and trace element analysis. A.S. performed the radiogenic isotope analyses. K.H. helped carry out field studies on Curaçao, contributed to the content of the manuscript and funded fieldwork and isotopic analyses.

Acknowledgements

Collection, analysis and publication of Curaçao samples and data was made possible due to NERC Fellowship NE/J019372/1 awarded to Alan R. Hastie and funds from the IFM-GEOMAR Leibniz Institute of Marine Sciences and GEOMAR Helmholtz Centre for Kaj Hoernle and DFG grant HO1833/22-1. Matthew Loewen and Robert Duncan are thanked for help in the field, posting samples back and for providing sample material for isotopic analyses. Catherine Chauvel is thanked for useful comments on a previous draft of the paper that highlighted to us the importance of fully explaining how we used the equations from Shaw (1970). Bernard Marty and Esteban Gazel are thanked for all their helpful comments and input.

Appendix A. Supplementary material

Supplementary material related to this article can be found online at http://dx.doi.org/10.1016/j.epsl.2016.03.023.

References

Allègre, C.J., Poirier, J.-P., Humler, E., Hofmann, A.W., 1995. The chemical composition of the Earth. Earth Planet. Sci. Lett. 134, 515–526.
Beets, D.J., 1972. Lithology and stratigraphy of the Cretaceous and Danian succession of Curaçao. PhD thesis. University of Amsterdam, Natuurwet Studiekring Sur and Netherlands Antilles, Amsterdam.
Beets, D.J., 1977. Cretaceous and Early Tertiary of Curaçao. In: 8th Caribbean Geological Conference Guide to Field Excursions. In: GUA Pap. Geol., Amsterdam, vol. 10, pp. 1–17.
Boyet, M., Carlson, R.W., 2006. A new geochemical model for the Earth's mantle inferred from ^{146}Sm–^{142}Nd systematics. Earth Planet. Sci. Lett. 250, 254–268.
Campbell, I.H., 2007. Testing the plume theory. Chem. Geol. 241, 153–176.
Cann, J.R., 1970. Rb, Sr, Y, Zr and Nb in some ocean floor basaltic rocks. Earth Planet. Sci. Lett. 10, 7–11.
Caro, G., Bourdon, B., 2010. Non-chondritic Sm/Nd ratio in the terrestrial planets: consequences for the geochemical evolution of the mantle–crust system. Geochim. Cosmochim. Acta 74, 3333–3349.
Coffin, M.F., Eldholm, O., 1994. Large igneous provinces: crustal structure, dimensions, and external consequences. Rev. Geophys. 32, 1–36.
Coogan, L.A., Saunders, A.D., Wilson, R.N., 2014. Aluminum-in-olivine thermometry of primitive basalts: evidence of an anomalously hot mantle source for large igneous provinces. Chem. Geol. 368, 1–10.
Farnetani, C.G., Samuel, H., 2005. Beyond the thermal plume paradigm. Geophys. Res. Lett. 32, L07311. http://dx.doi.org/10.1029/2005GL022360.
Farnetani, C.G., Legras, B., Tackley, P.J., 2002. Mixing and deformations in mantle plumes. Earth Planet. Sci. Lett. 196, 1–15.
Fitton, J.G., Saunders, A.D., Norry, M.J., Hardarson, B.S., Taylor, R.N., 1997. Thermal and chemical structure of the Iceland plume. Earth Planet. Sci. Lett. 153, 197–208.

Fitton, J.G., Godard, M., 2004. Origin and evolution of magmas on the OJP. In: Fitton, J.G., Mahoney, J.J., Wallace, P.J., Saunders, A.D. (Eds.), Origin and Evolution of the Ontong Java Plateau. In: Geol. Soc. (Lond.) Spec. Publ., vol. 229, pp. 151–178.

Fitton, J.G., 2007. The OIB paradox. In: Foulger, G.R., Jurdy, D.M. (Eds.), Plates, Plumes, and Planetary Processes. In: Spec. Pap., Geol. Soc. Am., vol. 430, pp. 387–412.

French, S.W., Romanowicz, B., 2015. Broad plumes rooted at the base of the Earth's mantle beneath major hotspots. Nature 525, 95–99.

Geldmacher, J., Hanan, B.B., Blichert-Toft, J., Harpp, K., Hoernle, K., Hauff, F., Werner, R., Kerr, A.C., 2003. Hafnium isotopic variations in volcanic rocks from the Caribbean Large Igneous Province and Galápagos hotspot tracks. Geochem. Geophys. Geosyst. 4 (7), 1062. http://dx.doi.org/10.1029/2002GC000477.

Graham, D.W., Larsen, L.M., Hanan, B.B., Storey, M., Pedersen, A.K., Lupton, J.E., 1998. Helium isotope composition of the early Iceland mantle plume inferred from the Tertiary picrites of West Greenland. Earth Planet. Sci. Lett. 160, 241–255.

Gudfinnsson, G.H., Presnall, D.C., 1996. Melting relations of model lherzolite in the system CaO–MgO–Al_2O_3–SiO_2 at 2.4–3.4 GPa and the generation of komatiites. J. Geophys. Res. 101, 27701–27709.

Hart, S.R., 1988. Heterogeneous mantle domains: signatures, genesis and mixing chronologies. Earth Planet. Sci. Lett. 90, 273–296.

Hart, S.R., Hauri, E.H., Oschmann, L.A., Whitehead, J.A., 1992. Mantle plumes and entrainment: isotopic evidence. Science 256, 517–520.

Hastie, A.R., Kerr, A.C., Pearce, J.A., Mitchell, S.F., 2007. Classification of altered island arc rocks using immobile trace elements: development of the Th–Co discrimination diagram. J. Petrol. 48, 2341–2357.

Hastie, A.R., Kerr, A.C., Mitchell, S.F., Millar, I., 2008. Geochemistry and petrogenesis of Cretaceous oceanic plateau lavas in eastern Jamaica. Lithos 101, 323–343.

Hastie, A.R., Kerr, A.C., 2010. Mantle plume or slab window?: physical and geochemical constraints on the origin of the Caribbean oceanic plateau. Earth-Sci. Rev. 98, 283–293.

Hastie, A.R., Mitchell, S.F., Kerr, A.C., Minifie, M.J., Millar, I.L., 2011. Geochemistry of rare high-Nb basalt lavas: are they derived from a mantle wedge metasomatised by slab melts? Geochim. Cosmochim. Acta 75, 5049–5072.

Hauff, F., Hoernle, K., Schmincke, H.-U., Werner, R., 1997. A mid cretaceous origin for the Galápagos hotspot: volcanological, petrological, and geochemical evidence from Costa Rican oceanic crustal segments. Geol. Rundsch. 86, 141–155.

Hauff, F., Hoernle, K.A., Tilton, G., Graham, D., Kerr, A.C., 2000a. Large volume recycling of oceanic lithosphere: geochemical evidence from the Caribbean Large Igneous province. Earth Planet. Sci. Lett. 174, 247–263.

Hauff, F., Hoernle, K.A., Bogaard, P.v.d., Alvarado, G.E., Garbe-Schönberg, D., 2000b. Age and geochemistry of basaltic complexes in Western Costa Rica: contributions to the Geotectonic Evolution of Central America. Geochem. Geophys. Geosyst. 1. http://dx.doi.org/10.1029/1999GC000020.

Hauri, E.H., Whitehead, J.A., Hart, S.R., 1994. Fluid dynamic and geochemical aspects of entrainment in mantle plumes. J. Geophys. Res. 99, 24,275–24,300.

Herzberg, C., O'Hara, M.J., 2002. Plume-associated ultramafic magmas of Phanerozoic age. J. Petrol. 43, 1857–1883.

Herzberg, C., 2004. Partial melting below the OJP. In: Fitton, J.G., Mahoney, J.J., Wallace, P.J., Saunders, A.D. (Eds.), Origin and Evolution of the OJP. In: Geol. Soc. (Lond.) Spec. Publ., vol. 229, pp. 179–183.

Herzberg, C., Asimow, P.D., Arndt, N., Niu, Y., Lesher, C.M., Fitton, J.G., Cheadle, M.J., Saunders, A.D., 2007. Temperatures in ambient mantle and plumes: constraints from basalts, picrites, and komatiites. Geochem. Geophys. Geosyst. 8. http://dx.doi.org/10.1029/2006GC001390.

Herzberg, C., Asimow, P.D., 2008. Petrology of some oceanic island basalts: PRIMELT2.XLS software for primary magma calculation. Geochem. Geophys. Geosyst. 9 (9). http://dx.doi.org/10.1029/2008GC002057.

Herzberg, C., Gazel, E., 2009. Petrological evidence for secular cooling in mantle plumes. Nature 458, 619–623.

Herzberg, C., Asimow, P.D., 2015. PRIMELT3 MEGA.XLSM software for primary magma calculation: peridotite primary magma MgO contents from the liquidus to the solidus. Geochem. Geophys. Geosyst. 16. http://dx.doi.org/10.1002/2014GC005631.

Hirose, K., Kushiro, I., 1993. Partial melting of dry peridotites at high pressures: determination of compositions of melts segregated from peridotite using aggregates of diamond. Earth Planet. Sci. Lett. 114, 477–489.

Hoernle, K.A., Bogaard, P.v.d., Werner, R., Lissinna, B., Hauff, F., Alvarado, G., Garbe-Schönberg, D., 2002. The missing history (16–71 Ma) of the Galápagos hotspot: implications for the Tectonic and Biological Evolution of the Americas. Geology 30, 795–798.

Hoernle, K., Hauff, F., Bogaard, P.v.d., 2004. A 70 Myr history (139–69 Ma) for the Caribbean large igneous province. Geology 32, 697–700.

Hoernle, K., Rohde, J.K., Hauff, F., Garbe-Schönberg, D., Homrighausen, S., Werner, R., Morgan, J.P., 2015. How and when plume zonation appeared during the 132 Myr evolution of the Tristan Hotspot. Nat. Commun. 6, 7799. http://dx.doi.org/10.1038/ncomms8799.

Hofmann, A.W., White, W.M., 1982. Mantle plumes from ancient oceanic crust. Earth Planet. Sci. Lett. 57, 421–436.

Hofmann, A.W., 1988. Chemical differentiation of the Earth: the relationship between mantle, continental crust, and oceanic crust. Earth Planet. Sci. Lett. 90, 297–314.

Ito, G., Mahoney, J.J., 2005. Flow and melting of a heterogeneous mantle. 1: method and importance to the geochemistry of ocean island and mid-ocean ridge basalts. Earth Planet. Sci. Lett. 230, 29–46.

Jackson, M.G., Hart, S.R., Saal, A.E., Shimizu, N., Kurz, M.D., Blusztajn, J.S., Skovgaard, A.C., 2008. Globally elevated titanium, tantalum, and niobium (TITAN) in ocean island basalts with high $^3He/^4He$. Geochem. Geophys. Geosyst. 9 (4). http://dx.doi.org/10.1029/2007GC001876.

Jackson, M.G., Carlson, R.W., Kurz, M.D., Kempton, P.D., Francis, D., Blusztajn, J., 2010. Evidence for the survival of the oldest terrestrial mantle reservoir. Nature 466, 853–856.

Jackson, M.G., Carlson, R.W., 2011. An ancient recipe for flood-basalt genesis. Nature 476, 316–319.

Jackson, M.G., Jellinek, A.M., 2013. Major and trace element composition of the high $^3He/^4He$ mantle: implications for the composition of a nonchondritic Earth. Geochem. Geophys. Geosyst. 14, 2954–2976. http://dx.doi.org/10.1002/ggge.20188.

Jackson, M.G., Cabral, R.A., Rose-Koga, E.F., Koga, K.T., Price, A., Hauri, E.H., Michael, P., 2015. Ultra-depleted melts in olivine-hosted melt inclusions from the Ontong Java Plateau. Chem. Geol. 414, 124–137.

Johnson, K.T.M., 1998. Experimental determination of partition coefficients for rare earth and high-field-strength elements between clinopyroxene, garnet, and basaltic melt at high pressures. Contrib. Mineral. Petrol. 133, 60–68.

Kempton, P.D., Fitton, J.G., Saunders, A.D., Nowell, G.M., Taylor, R.N., Hardarson, B.S., Pearson, G., 2000. The Iceland plume in space and time: a Sr–Nd–Pb–Hf study of the North Atlantic rifted margin. Earth Planet. Sci. Lett. 177, 255–271.

Kerr, A.C., Saunders, A.D., Tarney, J., Berry, N.H., Hards, V.L., 1995. Depleted mantle-plume geochemical signatures: no paradox for plume theories. Geology 23, 843–846.

Kerr, A.C., Tarney, J., Marriner, G.F., Klaver, G.T., Saunders, A.D., Thirlwall, M.F., 1996. The geochemistry and petrogenesis of the late-Cretaceous picrites and basalts of Curaçao, Netherlands Antilles: a remnant of an oceanic plateau. Contrib. Mineral. Petrol. 124, 29–43.

Kerr, A.C., 1998. Oceanic plateau formation: a cause of mass extinction and black shale deposition around the Cenomanian–Turonian boundary. J. Geol. Soc. Lond. 155, 619–626.

Kerr, A.C., Arndt, N.T., 2001. A note on the IUGS reclassification of the high-Mg and picritic volcanic rocks. J. Petrol. 42, 2169–2171.

Kerr, A.C., 2014. Oceanic plateaus. In: Holland, H., Turekian, K. (Eds.), Treatise on Geochemistry, 2nd ed. In: The Cust, vol. 4. Elsevier, Amsterdam, pp. 631–667.

Kinzler, R.J., 1997. Melting of mantle peridotite at pressures approaching the spinel to garnet transition: application to mid-ocean ridge basalt petrogenesis. J. Geophys. Res. 102, 853–874.

Klaver, G., 1987. The Curaçao lava formation: an ophiolitic analogue of the anomalously thick layer 2B of the mid-Cretaceous oceanic plateaux in the Western Pacific and central Caribbean. PhD thesis. University of Amsterdam.

Kokfelt, T.F., Hoernle, K., Hauff, F., Fiebig, J., Werner, R., Garbe-Schönberg, D., 2006. Combined trace element and Pb–Nd–Sr–O isotope evidence for recycled oceanic crust (upper and lower) in the Iceland mantle plume. J. Petrol. 47, 1705–1749.

Korenaga, J., Kelemen, P.B., 2000. Major element heterogeneity in the mantle source of the North Atlantic igneous province. Earth Planet. Sci. Lett. 184, 251–268.

Le Bas, M.J., Le Maitre, R.W., Woolley, A.R., 1992. The construction of the total alkali-silica chemical classification of volcanic rocks. Mineral. Petrol. 46, 1–22.

Le Bas, M.J., 2000. IUGS reclassification of the high-Mg and picritic volcanic rocks. J. Petrol. 41, 1467–1470.

Loewen, M.W., Duncan, R.A., Kent, A.J.R., Krawl, K., 2013. Prolonged plume volcanism in the Caribbean Large Igneous Province: new insights from Curaçao and Haiti. Geochem. Geophys. Geosyst. 14 (10), 4241–4259. http://dx.doi.org/10.1002/ggge.20273.

Lohmann, F.C., Hort, M., Morgan, J.P., 2009. Flood basalts and ocean island basalts: a deep source or shallow entrainment? Earth Planet. Sci. Lett. 284, 553–563.

McDonald, I., Viljoen, K.S., 2006. Platinum-group element geochemistry of mantle eclogites: a reconnaissance study of xenoliths from the Orapa kimberlite, Botswana. Trans. - Inst. Min. Metall., B, Appl. Earth Sci. 115, 81–93.

McDonough, W.F., Sun, S.-s., 1995. The composition of the Earth. Chem. Geol. 120, 223–253.

McDonough, W.F., 2001. The composition of the Earth. In: Teisseyre, R., Majewski, E. (Eds.), Earthquake Thermodynamics and Phase Transformations in the Earth's Interior. In: Int. Geophys. Ser., vol. 76, pp. 3–23.

Neill, I., Gibbs, J.A., Hastie, A.R., Kerr, A.C., 2010. Origin of the volcanic complexes of La Désirade, Lesser Antilles: implications for tectonic reconstruction of the Late Jurassic to Cretaceous Pacific-proto Caribbean margin. Lithos 120, 407–420.

Pearce, J.A., 1996. A users guide to basalt discrimination diagrams. In: Wyman, D.A. (Ed.), Trace Element Geochemistry of Volcanic Rocks: Applications for Massive Sulphide Exploration. In: Geological Association Canada Short Course Notes, vol. 12, pp. 79–113.

Phipps Morgan, J., Morgan, W.J., 1999. Two-stage melting and the geochemical evolution of the mantle: a recipe for mantle plum-pudding. Earth Planet. Sci. Lett. 170, 215–239.

Pilet, S., Baker, M.B., Müntener, O., Stolper, E.M., 2011. Monte Carlo simulations of metasomatic enrichment in the Lithosphere and implications for the source of alkaline basalts. J. Petrol. 52, 1415–1442.

Reichow, M.K., Pringle, M.S., Al'Mukhamedov, A.I., Allen, M.B., Andreichev, V.L., Buslov, M.M., Davies, C.E., Fedoseev, G.S., Fitton, J.G., Inger, S., Medvedev, A.Ya., Mitchell, C., Puchkov, V.N., Safonova, I.Yu., Scott, R.A., Saunders, A.D., 2009. The timing and extent of the eruption of the Siberian Traps large igneous province: implications for the end-Permian environmental crisis. Earth Planet. Sci. Lett. 277, 9–20.

Ringwood, A.E., 1962. A model for the upper mantle. J. Geophys. Res. 67, 857–867.

Salters, V.J.M., Zindler, A., 1995. Extreme $^{176}Hf/^{177}Hf$ in the sub-oceanic mantle. Earth Planet. Sci. Lett. 129, 13–30.

Salters, V.J.M., Stracke, A., 2004. Composition of the depleted mantle. Geochem. Geophys. Geosyst. 5, Q05B07. http://dx.doi.org/10.1029/2003GC000597.

Schilling, J.G., 1973. Iceland mantle plume: geochemical study of Reykjanes Ridge. Nature 242, 565–571.

Schubert, G., Sandwell, D., 1989. Crustal volumes of the continents and of oceanic and continental submarine plateaus. Earth Planet. Sci. Lett. 92, 234–246.

Shaw, D.M., 1970. Trace element fractionation during anatexis. Geochim. Cosmochim. Acta 34, 237–243.

Skovgaard, A.C., Storey, M., Baker, J., Blusztajn, J., Hart, S.R., 2001. Osmium–oxygen isotopic evidence for a recycled and strongly depleted component in the Iceland mantle plume. Earth Planet. Sci. Lett. 194, 259–275.

Sobolev, A.V., Hofmann, A.W., Sobolev, S.V., Nikogosian, I.K., 2005. An olivine-free mantle source of Hawaiian shield basalts. Nature 434, 590–597.

Starkey, N.A., Fitton, J.G., Stuart, F.M., Larsen, L.M., 2012. Melt inclusions in olivines from early plume picrites support high $^{3}He/^{4}He$ in both enriched and depleted mantle. Chem. Geol. 306–307, 54–62.

Stuart, F.M., Lass-Evans, S., Fitton, J.G., Ellam, R.M., 2003. High $^{3}He/^{4}He$ ratios in picritic basalts from Baffin Island and the role of a mixed reservoir in mantle plumes. Nature 424, 57–59.

Sun, S.-s., 1982. Chemical composition and origin of the earth's primitive mantle. Geochim. Cosmochim. Acta 46, 179–192.

Sun, S-s., McDonough, W.F., 1989. Chemical and isotopic systematics of oceanic basalts: implications for mantle composition and processes. Geol. Soc. (Lond.) Spec. Publ. 42, 313–345.

Tejada, M.L.G., Mahoney, J.J., Neal, C.R., Duncan, R.A., Petterson, M.G., 2002. Basement geochemistry and geochronology of central Malaita, Solomon Islands, with implications for the origin and evolution of the Ontong Java Plateau. J. Petrol. 43, 449–484.

Tejada, M.L.G., Mahoney, J.J., Castillo, P.R., Ingle, S.P., Sheth, H.C., Weis, D., 2004. Pin-pricking the elephant: evidence on the origin of the OJP from Pb–Sr–Hf–Nd isotopic characteristics of ODP Leg 192 basalts. In: Fitton, J.G., Mahoney, J.J., Wallace, P.J., Saunders, A.D. (Eds.), Origin and Evolution of the OJP. In: Geol. Soc. (Lond.) Spec. Publ., vol. 229, pp. 133–150.

Thompson, P.M.E., Kempton, P.D., White, R.V., Kerr, A.C., Tarney, J., Saunders, A.D., Fitton, J.G., 2003. Hf–Nd isotope constraints on the origin of the Cretaceous Caribbean plateau and its relationship to the Galapagos plume. Earth Planet. Sci. Lett. 217, 59–75.

Trela, J., Vidito, C., Gazel, E., Herzberg, C., Class, C., Whalen, W., Jicha, B., Bizimis, M., Alvarado, G.E., 2015. Recycled crust in the Galápagos Plume source at 70 Ma: implications for plume evolution. Earth Planet. Sci. Lett. 425, 268–277.

Walter, M.J., 1998. Melting of garnet peridotite and the origin of komatiite and depleted lithosphere. J. Petrol. 39, 29–60.

West Jr., D.P., Abbott Jr., R.N., Bandy, B.R., Kunk, M., 2014. Protolith provenance and thermotectonic history of metamorphic rocks in eastern Jamaica: evolution of a transform plate boundary. Geol. Soc. Am. Bull. 126, 600–614.

White, R.V., Saunders, A.D., 2005. Volcanism, impact and mass extinctions: incredible or credible coincidences? Lithos 79, 299–316.

Wignall, P.B., 2001. Large igneous provinces and mass extinctions. Earth Planet. Sci. Lett. 53, 1–33.

Winchester, J.A., Floyd, P.A., 1977. Geochemical discrimination of different magma series and their differentiation products using immobile elements. Chem. Geol. 20, 325–343.

Workman, R.K., Hart, S.R., Jackson, M., Regelous, M., Farley, K.A., Blusztajn, J., Kurz, M., Staudigel, H., 2004. Recycled metasomatised lithosphere as the origin of the enriched mantle II (EM2) end-member: evidence from the Samoan Volcanic Chain. Geochem. Geophys. Geosyst. 5. http://dx.doi.org/10.1029/2003GC000623.

Workman, R.K., Hart, S.R., 2005. Major and trace element composition of the depleted MORB mantle (DMM). Earth Planet. Sci. Lett. 231, 53–72.

Zindler, A., Hart, S.R., 1986. Chemical geodynamics. Annu. Rev. Earth Planet. Sci. 14, 493–571.